Supporting information for:

Conformational differences of the C8-deoxyguanosine adduct of 2-amino-3-methylimidazo[4,5-f]quinoline (IQ) within the NarI recognition sequence

C. Eric Elmquist, Feng Wang, James S. Stover, Michael P. Stone,* Carmelo J. Rizzo*

Contribution from the Department of Chemistry, Center in Molecular Toxicology, Vanderbilt Institute of Chemical Biology, and Vanderbilt-Ingram Cancer Center, Vanderbilt University, VU Station B 351822, Nashville, Tennessee 37235-1822

Scheme S1

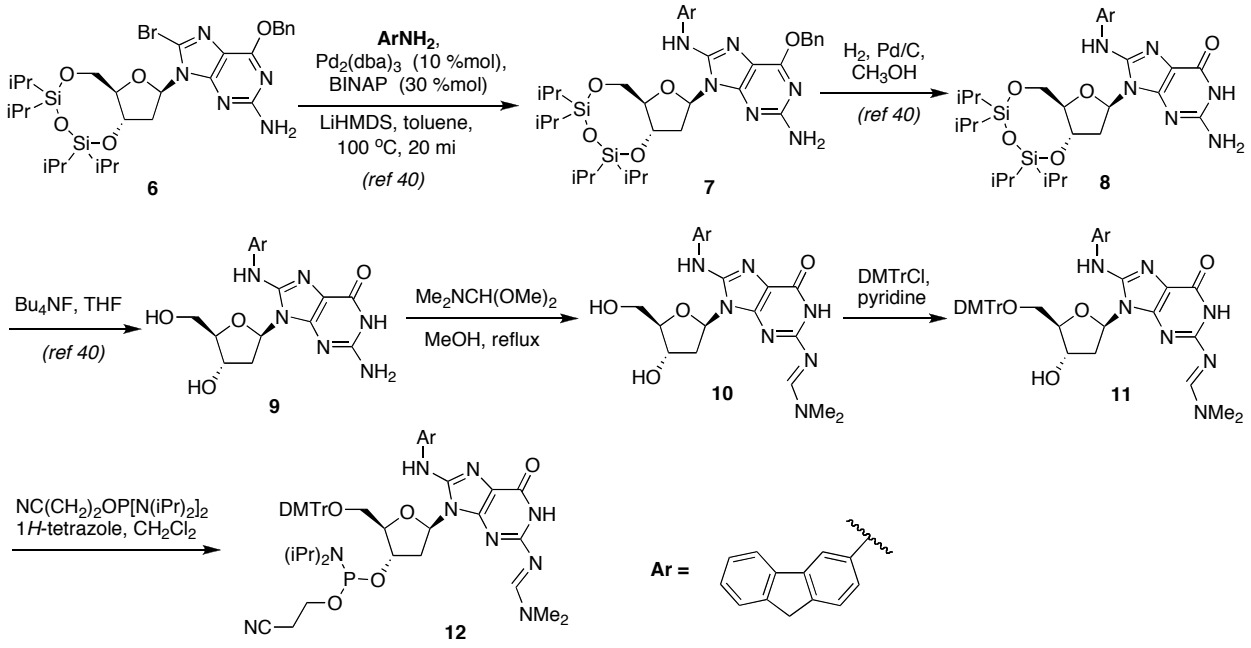

Chemicals. All commercially obtained chemicals were of the highest available purity and used as received unless noted otherwise. All chemicals were purchased from Aldrich (Milwaukee, WI) except 4,4'-dimethoxytrityl chloride which was purchased from ChemGenes Corp. (Wilmington, MA). 8-bromo-2-dGuo was purchased from Sigma (St. Louis, MO). Pyridine. methylene chloride and diisopropylethylamine were freshly distilled from calcium hydride. Anhydrous methanol was purchased from Aldrich in a Sure-seal bottle. Compounds **9** was prepared as previously reported (40). All reactions were performed in oven-dried glassware and under an argon atmosphere.

***N*^{2}-[(Dimethylamino)methylene]-8-(9*H*-fluoren-2-ylamin)-β-D-2'-deoxyribofuranosyl]-guanine (10).** To a stirred solution of **9** (100 mg, 0.224 mmol) in anhydrous methanol (2 mL) under and argon atmosphere was added *N,N*-dimethylformamide diethyl acetal (0.3 mL, 1.82 mmol). The reaction was heated to 50 °C and stirred for 2 h, after which time the reaction mixture was allowed to cool to room temperature. The solvent was evaporated under reduced

pressure and the residue purified by flash chromatography on silica, eluting with 5% methanol in methylene chloride to give **10** (111 mg, 99% yield) as a reddish-purple solid. mp 188-190 °C; $[\alpha]^{23}_{D}$ +120.0 ° (*c* 0.5, MeOH:CH_2Cl_2 = 1:1); ^{1}H NMR (DMSO-d_6) δ 11.30 (br s, 1H), 8.84 (s, 1H), 8.53 (s, 1H), 8.11 (s, 1H), 7.77 (dd, *J* = 7.4, 4.8, 2H), 7.67 (d, *J* = 8.7, 1H), 7.53 (d, *J* = 7.5, 1H), 7.33 (t, *J* = 7.3, 1H), 7.23 (q, *J* = 14.3, 7.1, 1H), 6.46 (dd, *J* = 8.8, 5.9, 1H), 5.96 (s, 1H), 5.41 (s, 1H), 4.47 (s, 1H), 3.94 (s, 1H), 3.90 (s, 2H), 3.78 (s, 2H), 3.15 (s, 3H), 3.02 (s, 3H), 2.66-2.57 (m, 1H), 2.49 (s, 1H), 2.11-2.05 (m, 1H); ^{13}C NMR (DMSO-d_6) δ 157.48, 156.55, 155.88, 148.11, 144.21, 143.75, 142.41, 141.33, 139.88, 134.12, 126.61, 125.48, 124.87, 119.94, 116.44, 115.62, 114.04, 87.19, 82.71, 71.06, 61.19, 40.52, 38.36, 36.50, 34.56; HRMS (FAB, NBA) *m/z* calcd for $C_{26}H_{27}N_7O_4$ (M^+H) 502.2203, found 502.2227.

***N*^{2}-[(Dimethylamino)methylene]-8-[9*H*-fluoren-2-ylamino]-*N*9[5'-*O*-[bis(4-methoxyphenyl)phenylmethyl]]-β-D-2'-deoxyribofuranosyl]guanine (11).** To a stirred solution of **10** (50 mg, 0.100 mmol) in anhydrous pyridine (0.8 mL) and freshly distilled diisopropylethylamine (0.105 mL) under an argon atmosphere, was added 4, 4'-dimethoxytrityl chloride (101 mg, 0.30 mmol) at 0 °C. The reaction was warmed to room temperature and stirred for 3 h. The solvent was evaporated under reduced pressure and the residue was purified by flash chromatography on silica, eluting with 2.5% methanol in methylene chloride containing 0.5% pyridine to give **11** (55 mg, 69% yield) as a light gray solid. mp 128-130 °C; $[\alpha]^{23}_{D}$ -12.0 ° (*c* 0.5, CH_2Cl_2); ^{1}H NMR (CD_2Cl_2) δ 9.15 (br s, 1H), 8.47 (s, 1H), 7.65 (d, *J* = 7.2, 1H), 7.52 (d, *J* = 8.0, 1H), 7.46 (d, *J* = 7.6, 1H), 7.40 (t, *J* = 7.2, 3H), 7.32-7.27 (m, 5H), 7.20 (t, *J* = 7.0, 3H), 7.16 (t, *J* = 8.8, 2H), 6.74 (d, *J* = 8.8, 4H), 6.37 (t, *J* = 6.8, 1H), 4.52-4.50 (m, 1H), 4.15 (q, *J* = 9.2, 4.8, 1H), 3.76 (s, 2H), 3.66 (s, 3H), 3.65 (s, 3H), 3.44 (d, *J* = 5.2, 2H), 3.04 (s, 3H), 3.00 (s, 3H), 2.90-2.83 (m, 2H), 2.41-2.36 (mm, 1H); ^{13}C NMR (CD_2Cl_2) δ 158.18, 157.03, 156.28,

154.81, 148.39, 145.19, 144.07, 143.95, 142.54, 141.17, 138.21, 134.98, 129.51, 129.45, 128.51, 127.58, 127.36, 127.16, 126.40, 126.06, 125.09, 124.30, 119.42, 118.41, 116.49, 115.95, 114.19, 112.62, 86.12, 85.18, 83.71, 71.46, 63.37, 54.58, 40.59, 38.58, 36.49, 34.29, 29.17; HRMS (FAB, NBA) *m/z* calcd for $C_{47}H_{45}N_7O_6$ (M+H) 804.3510, found 804.3528.

***N*^{2}-[(Dimethylamino)methylene]-8-[9*H*-fluoren-2-ylamino]-*N*9[5'-*O*-[bis(4-methoxyphenyl)phenylmethyl]-3'-*O*-[[bis(1-methylethylamino](2-cyanoethoxy)phosphino]]-β-D-2'-deoxyribofuranosyl]guanine (12).** To a stirred suspension of **11** (50 mg, 0.062 mmol) and 1*H*-tetrazole (5 mg, .07 mmol) in anhydrous methylene chloride (3 mL) was added 2-cyanoethyl tetraisopropylphosphorodiamidite (0.028 mL, 0.085 mmol) and the reaction was stirred for 1.5 h. Following removal of the solvent by evaporation under reduced pressure, the residue was purified by flash chromatography on silica, eluting with 2% methanol in methylene chloride containing 0.5% pyridine to give **12** (28 mg, 45% yield) as a light pink solid. mp 84-86 °C; $[\alpha]^{23}_{D}$ +8.8° (*c* 0.5, CH_2Cl_2); ^{1}H NMR (CD_2Cl_2) δ 8.84 (br s, 1H), 8.55 (s, 1H), 7.74 (d, *J* = 6.8, 1H), 7.67 (d, *J* = 7.6, 1H), 7.58-7.13 (mm, 15H), 6.77-6.70 (m, 4H), 6.35 (t, *J* = 8.0, 1H), 4.67-4.60 (m, 1H), 4.29-4.24 (m, 1H), 3.82-3.37 (mm, 14H), 3.12 (d, *J* = 3.2, 3H), 3.07 (s, 3H), 2.99-2.90 (m, 1H), 2.58-2.40 (mm, 3H), 1.24 (s, 1H), 1.52 (t, *J* = 7.4, 8H), 1.05 (d, *J* = 6.8, 3H); ^{13}C NMR (CD_2Cl_2) δ 159.25, 158.17, 157.05, 155.97, 149.29, 146.18, 145.09, 143.66, 142.25, 139.36, 136.14, 136.01, 135.94, 130.65, 130.56, 128.77, 128.70, 128.45, 127.50, 127.15, 126.21, 125.41, 124.49, 120.53, 119.52, 118.25, 117.75, 117.66, 117.17, 115.44, 115.35, 113.69, 87.15, 85.61, 85.56, 84.79, 84.70, 74.28, 74.14, 64.07, 58.93, 58.78, 55.66, 43.91, 43.82, 41.71, 38.56, 37.61, 35.43, 30.25, 24.96, 24.89, 24.84, 20.97, 20.91; HRMS (FAB, NBA) *m/z* calcd for $C_{56}H_{62}N_9O_7P$ (M+) 1004.4588, found 1004.4562.

Thermal melting studies. Equal amounts of the adducted and the complementary strands (0.3 units each) were dissolved in 0.5 mL of buffer (100 mM NaCl, .05 mM EDTA, and 10 mM phosphate buffer, pH 7.1). The UV absorption at 260 nm was monitored as a function of temperature. The temperature was increased at a rate of 1 °C/min from 5 to 90°C. The melting temperatures of the native and modified oligonucleotides were calculated by determining the first derivative of the melting curve. The cell path length was 1.0 cm.

Circular dichroism measurements. CD measurements were carried out with the same solutions as the T_m studies and at 23° C. Samples were scanned from 410.0–220.0 nm at 0.5 nm intervals averaged over 1 second in a 300 μL strain free quartz cuvette. The corresponding raw CD spectra were subtracted from a blank, converted to molar ellipticity, and processed using provided the manufacturer's software package.

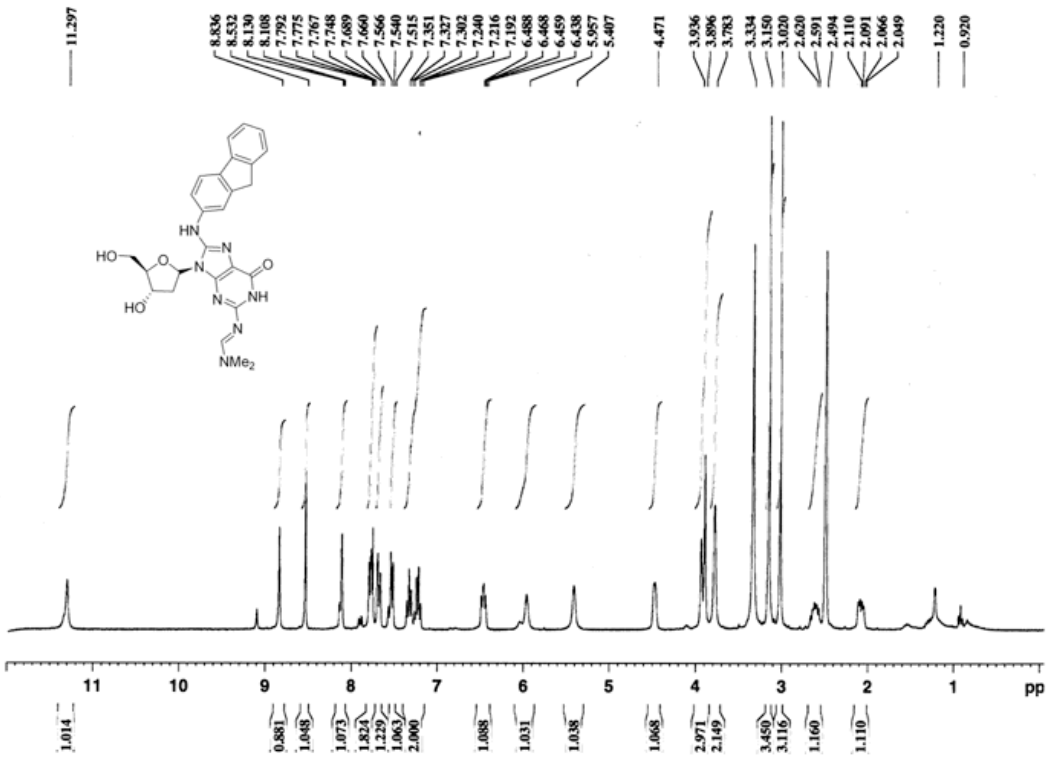

Figure S1. ^{1}H NMR spectrum of N^{2}-[(dimethylamino)methylene]-8-(9*H*-fluoren-2-ylamin)-β-D-2'-deoxyribofuranosyl]guanine (**10**)

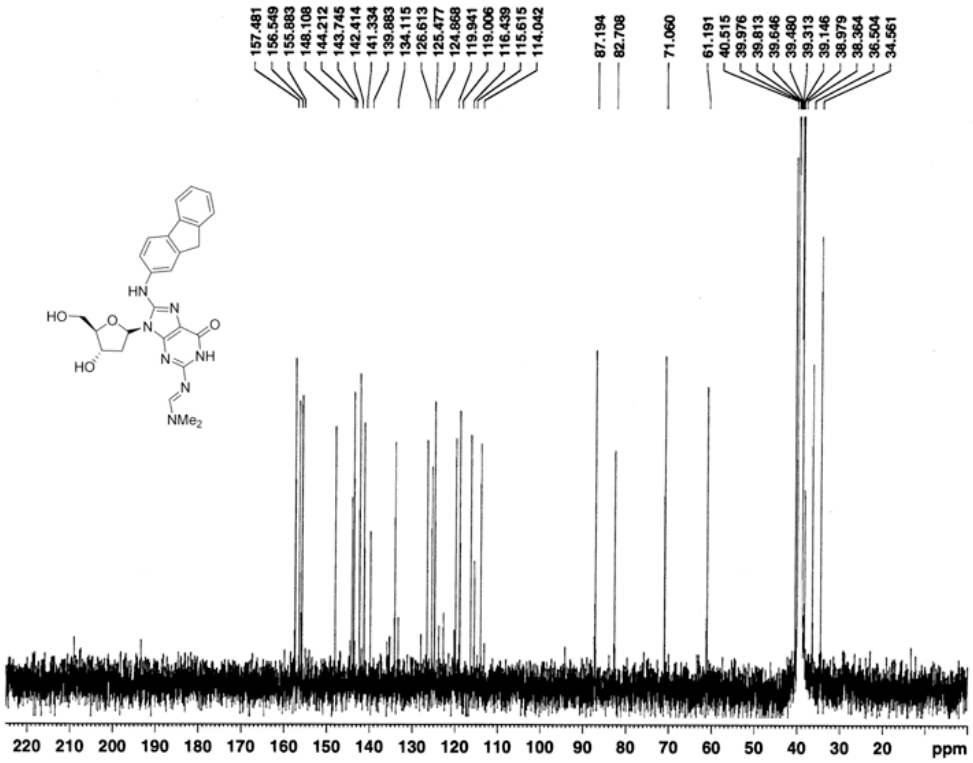

Figure S2. ^{13}C NMR spectrum of N^{2}-[(dimethylamino)methylene]-8-(9*H*-fluoren-2-ylamin)-β-D-2'-deoxyribofuranosyl]guanine (**10**)

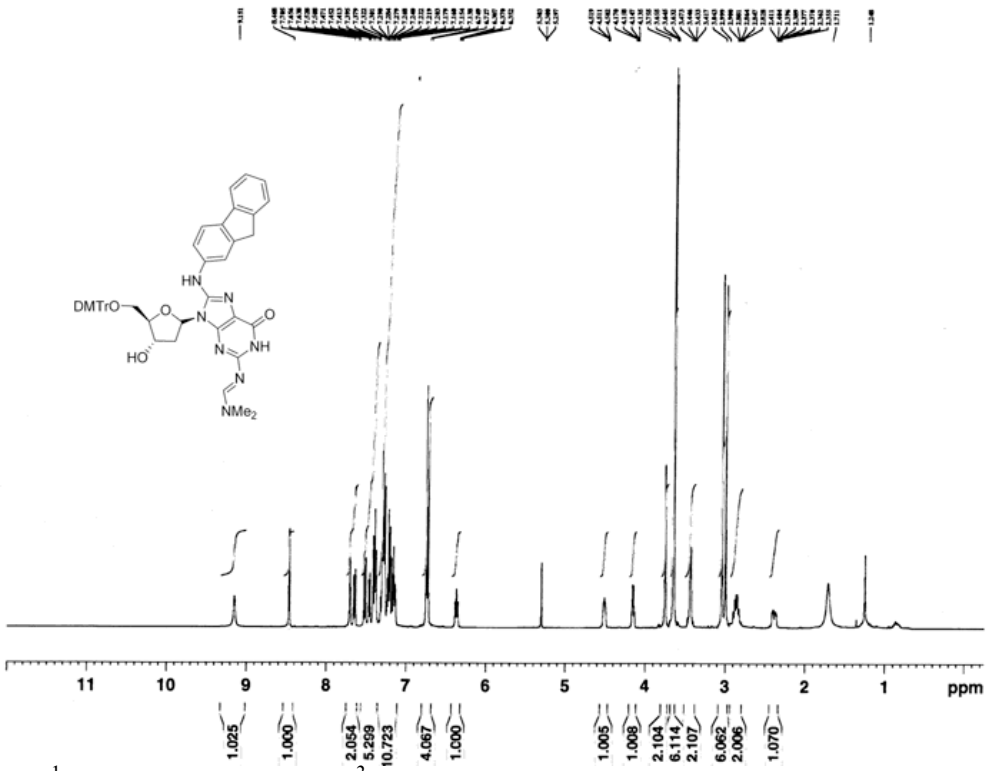

Figure S3. ^{1}H NMR spectrum of N^{2}-[(dimethylamino)methylene]-8-[9*H*-fluoren-2-ylamino]-*N*9[5'-*O*-[bis(4-methoxyphenyl)phenylmethyl]]-β-D-2'-deoxyribofuranosyl]guanine (**11**)

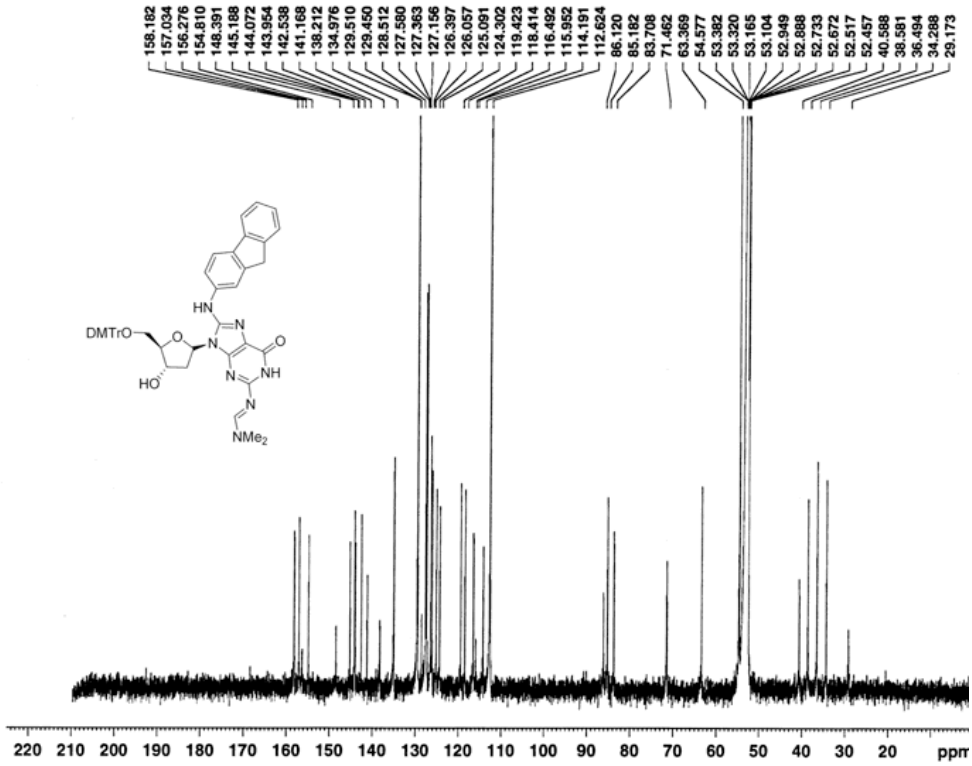

Figure S4. ^{13}C NMR spectrum of N^{2}-[(dimethylamino)methylene]-8-[9*H*-fluoren-2-ylamino]-*N*9[5'-*O*-[bis(4-methoxyphenyl)phenylmethyl]]-β-D-2'-deoxyribofuranosyl]guanine (**11**)

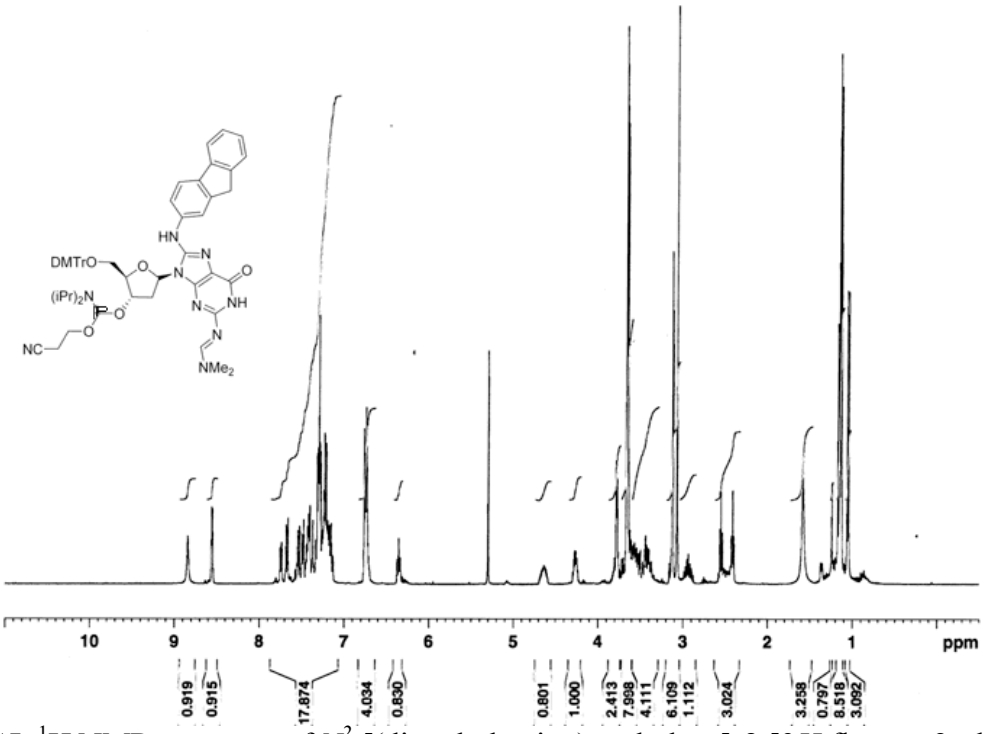

Figure S5. ^{1}H NMR spectrum of *N*^{2}-[(dimethylamino)methylene]-8-[9*H*-fluoren-2-ylamino]-*N*9[5'-*O*-[bis(4-methoxyphenyl)phenylmethyl]-3'-*O*-[[bis(1-methylethylamino](2-cyanoethoxy)phosphino]]-β-D-2'-deoxyribofuranosyl]guanine (**12**)

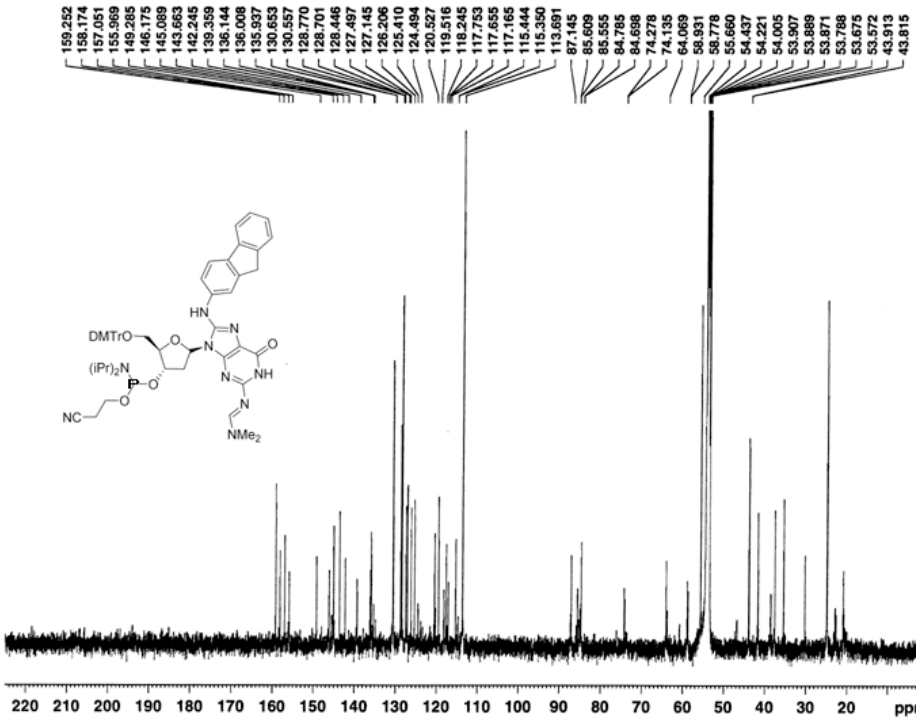

Figure S6. ^{13}C NMR spectrum of *N*^{2}-[(dimethylamino)methylene]-8-[9*H*-fluoren-2-ylamino]-*N*9[5'-*O*-[bis(4-methoxyphenyl)phenylmethyl]-3'-*O*-[[bis(1-methylethylamino](2-cyanoethoxy)phosphino]]-β-D-2'-deoxyribofuranosyl]guanine (**12**)

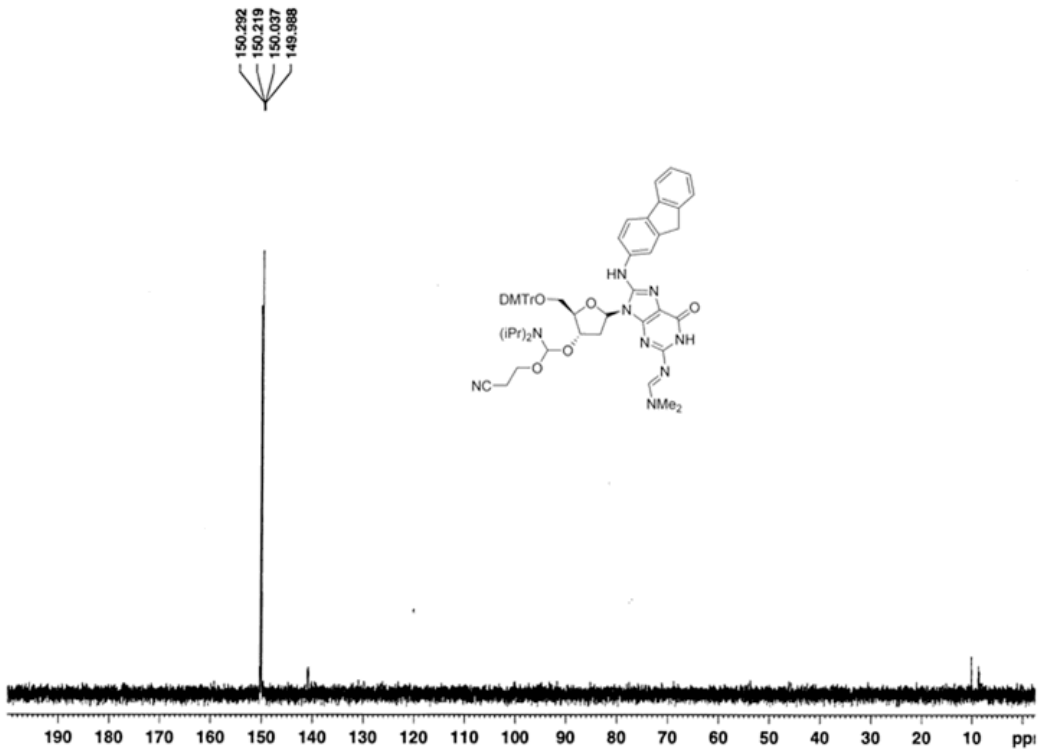

Figure S7. ^{31}P NMR spectrum of N^2-[(dimethylamino)methylene]-8-[9*H*-Fluoren-2-ylamino]-*N*9[5'-*O*-[bis(4-methoxyphenyl)phenylmethyl]-3'-*O*-[[bis(1-methylethylamino](2-cyanoethoxy)phosphino]]-β-D-2'-deoxyribofuranosyl]guanine (**12**)

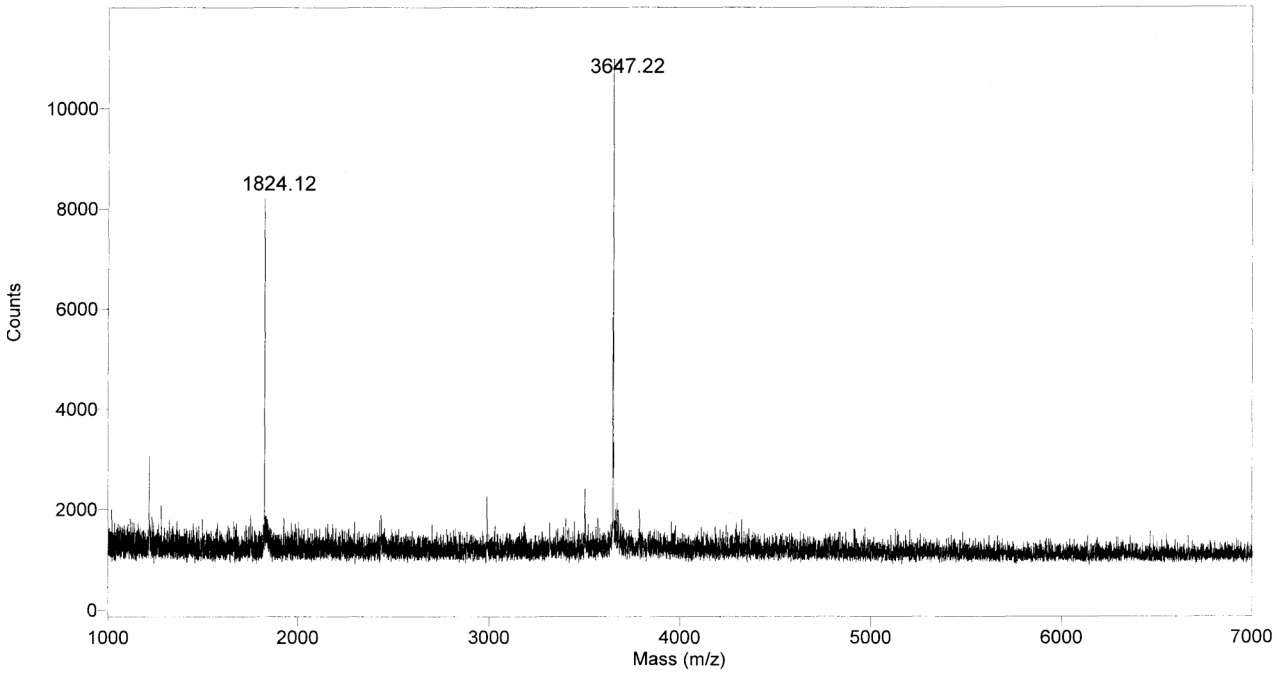

Figure S8. MALDI-TOF mass spectrum of 5'-d(GGCA-G^{IQ}-GTGGTG)-3' (**1a**)

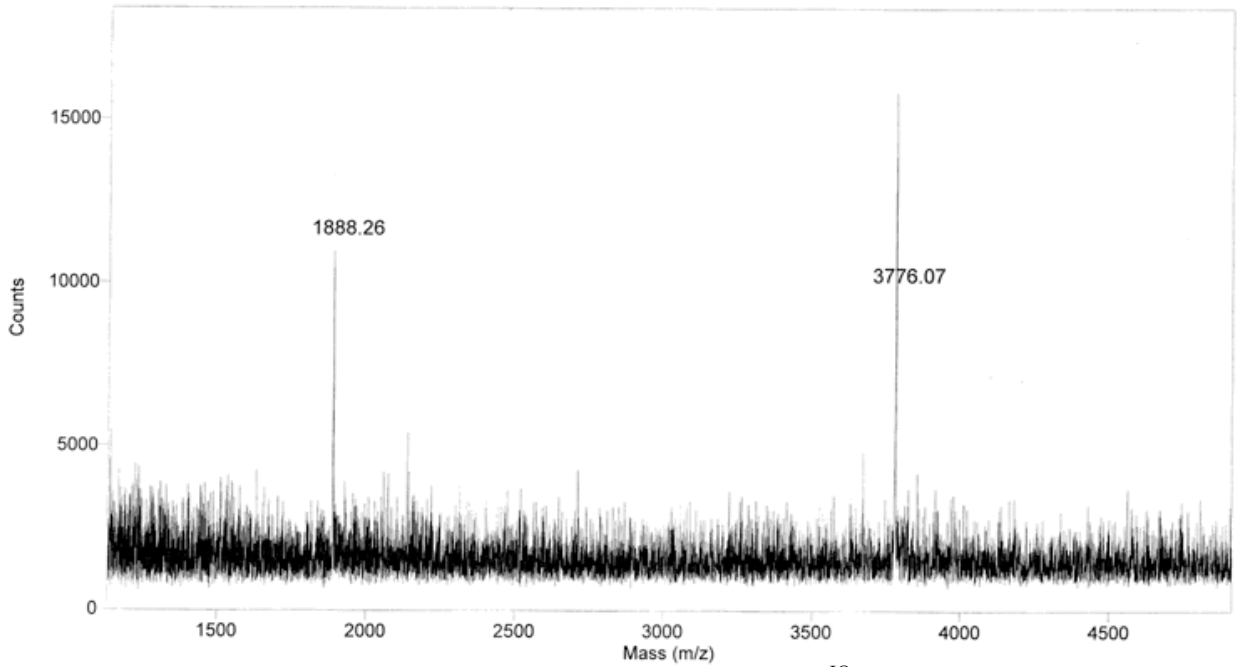

Figure S9. MALDI-TOF mass spectrum of 5'-d(CTC-G^{IQ}-GCGCCATC)-3' (**2a**)

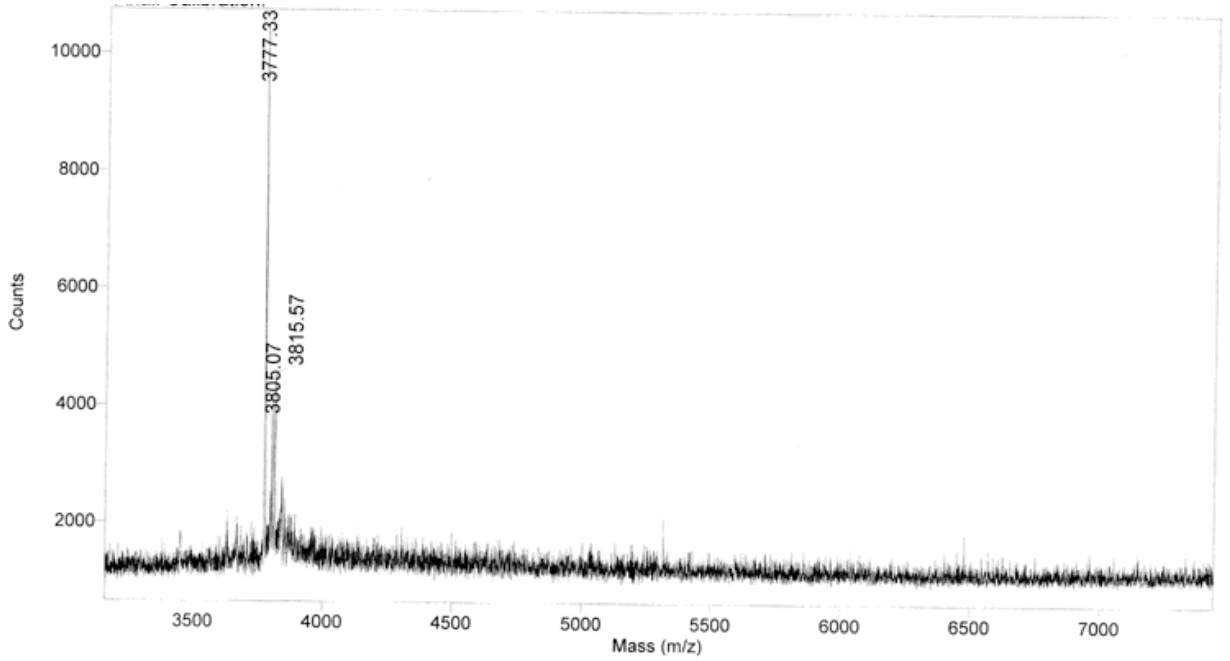

Figure S10. MALDI-TOF mass spectrum of 5'-d(CTCG-G^{IQ}-CGCCATC)-3' (**3a**)

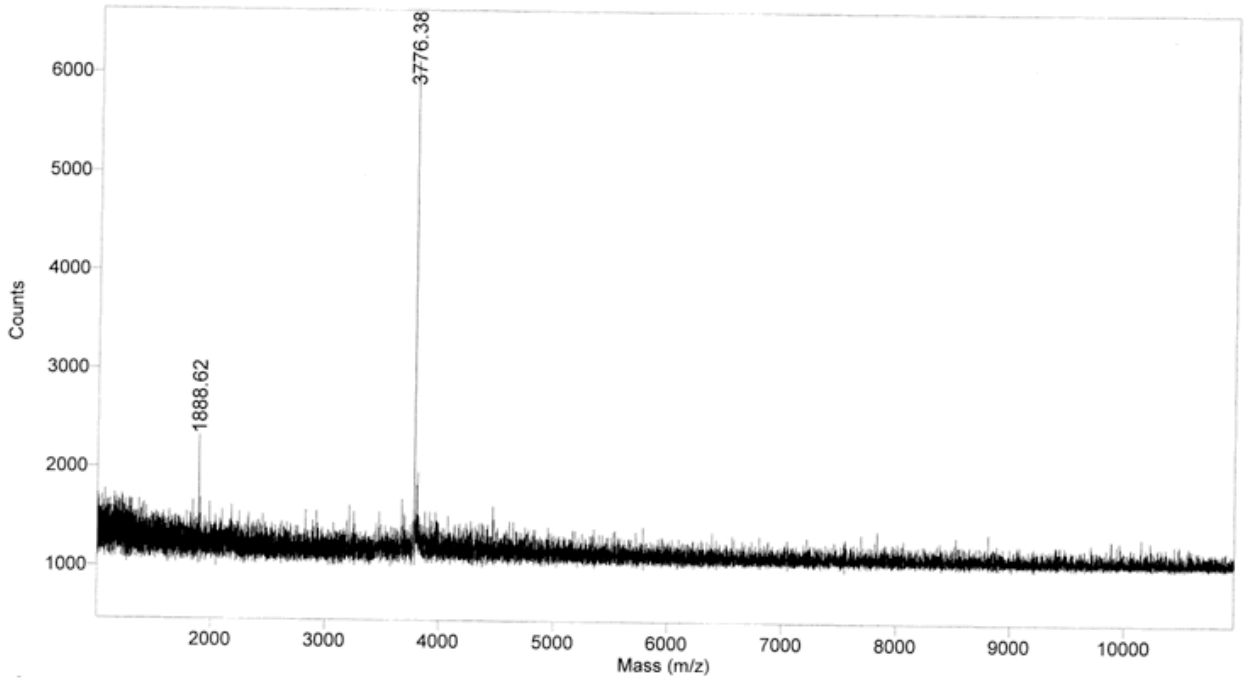

Figure S11. MALDI-TOF mass spectrum of 5'-d(CTCGGC-G^{IQ}-CCATC)-3' (**4a**)

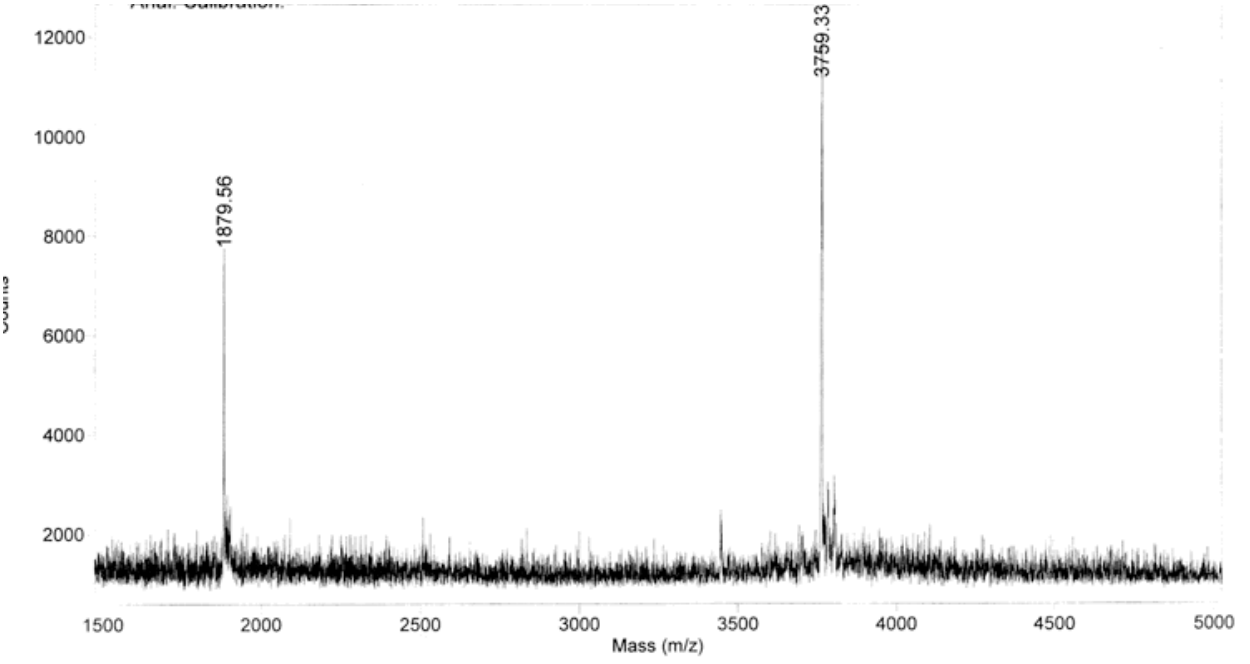

Figure S12. MALDI-TOF mass spectrum of 5'-d(CTC-G^{AF}-GCGCCATC)-3' (**2b**)

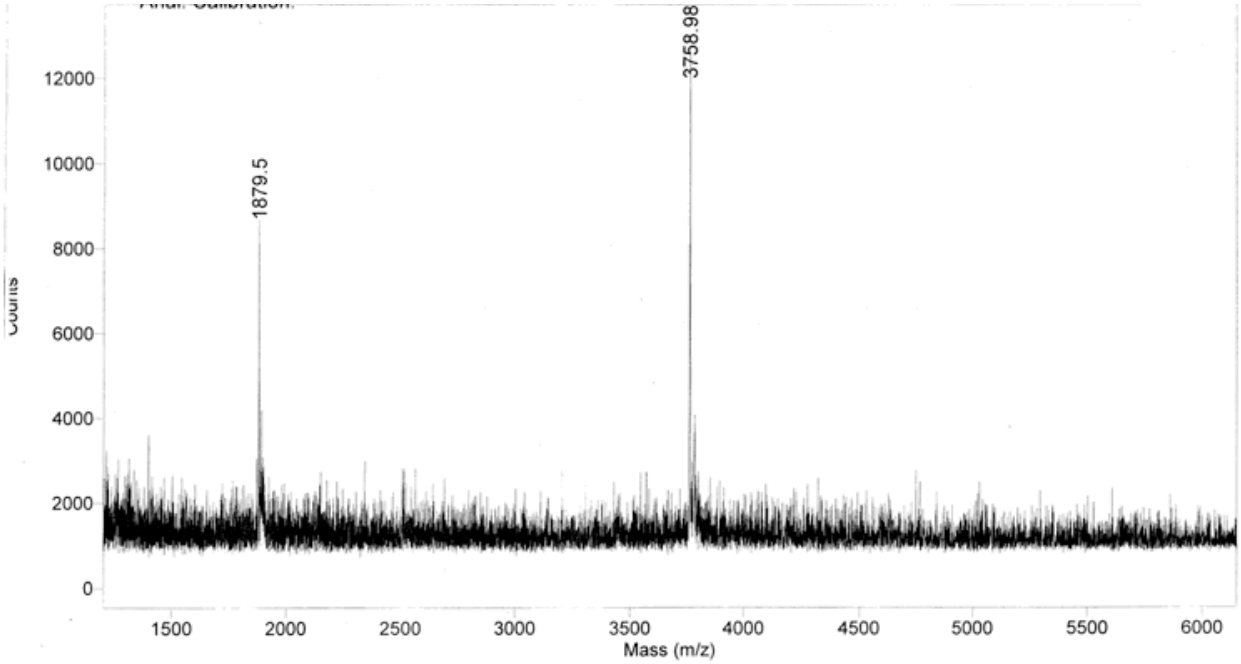

Figure S13. MALDI-TOF mass spectrum of 5'-d(CTCG-G^{AF}-CGCCATC)-3' (**3b**)

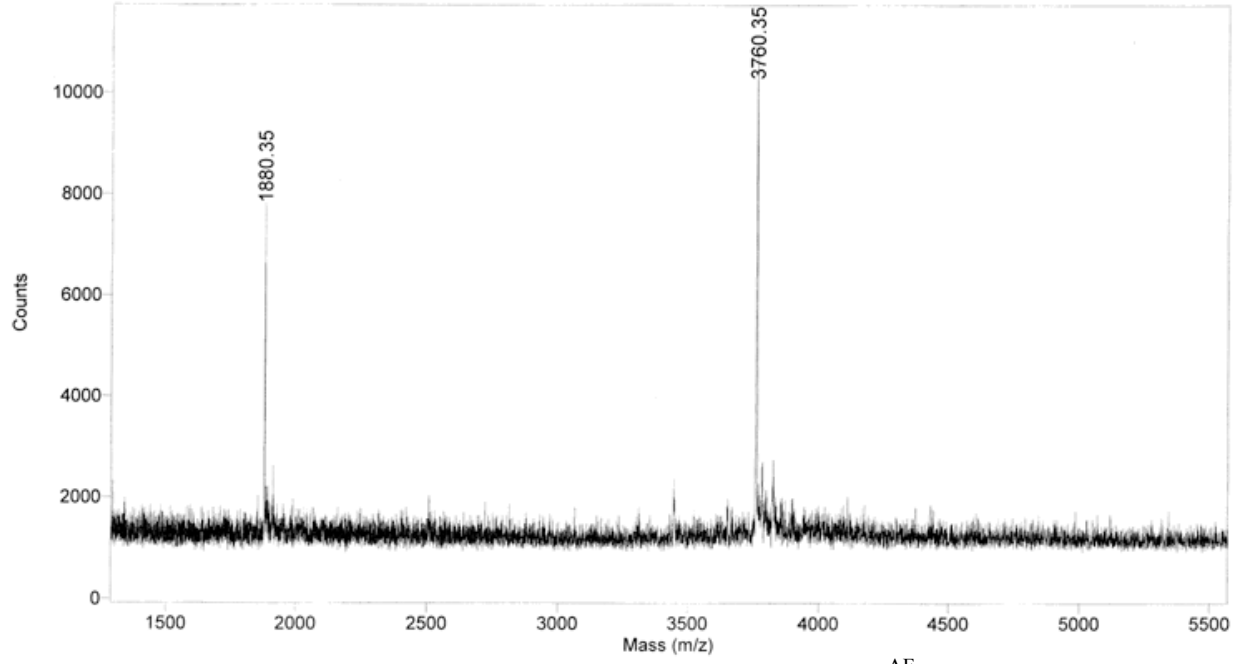

Figure S14. MALDI-TOF mass spectrum of 5'-d(CTCGGC-G^{AF}-CCATC)-3' (**4b**)

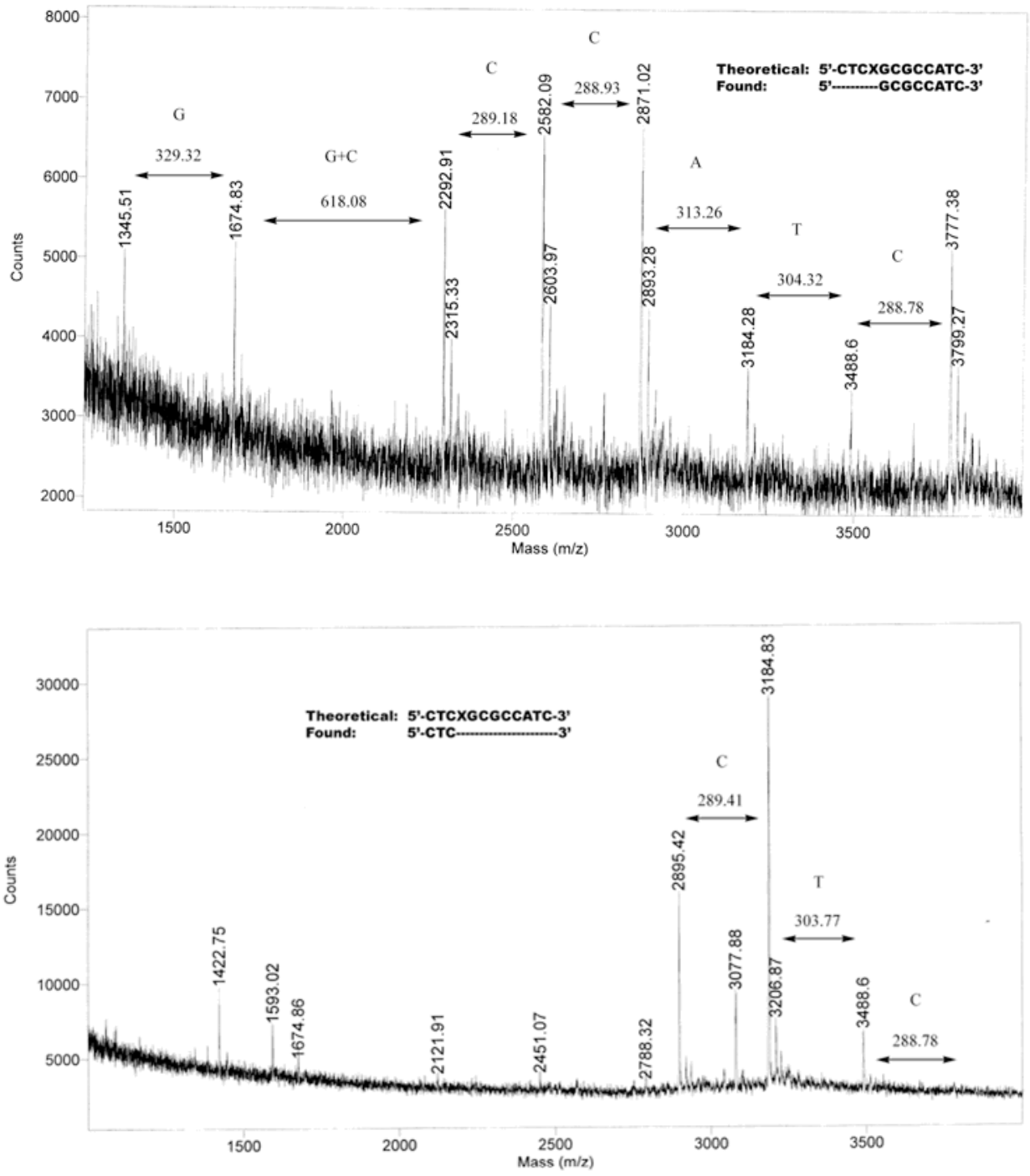

Figure S15. Sequencing of 5'-d(CTC-G^{IQ}-GCGCCATC)-3' (**2a**) by controlled digestion with phosphodiesterase I (top) or phosphodiesterase II (bottom) and MALDI-TOF analysis

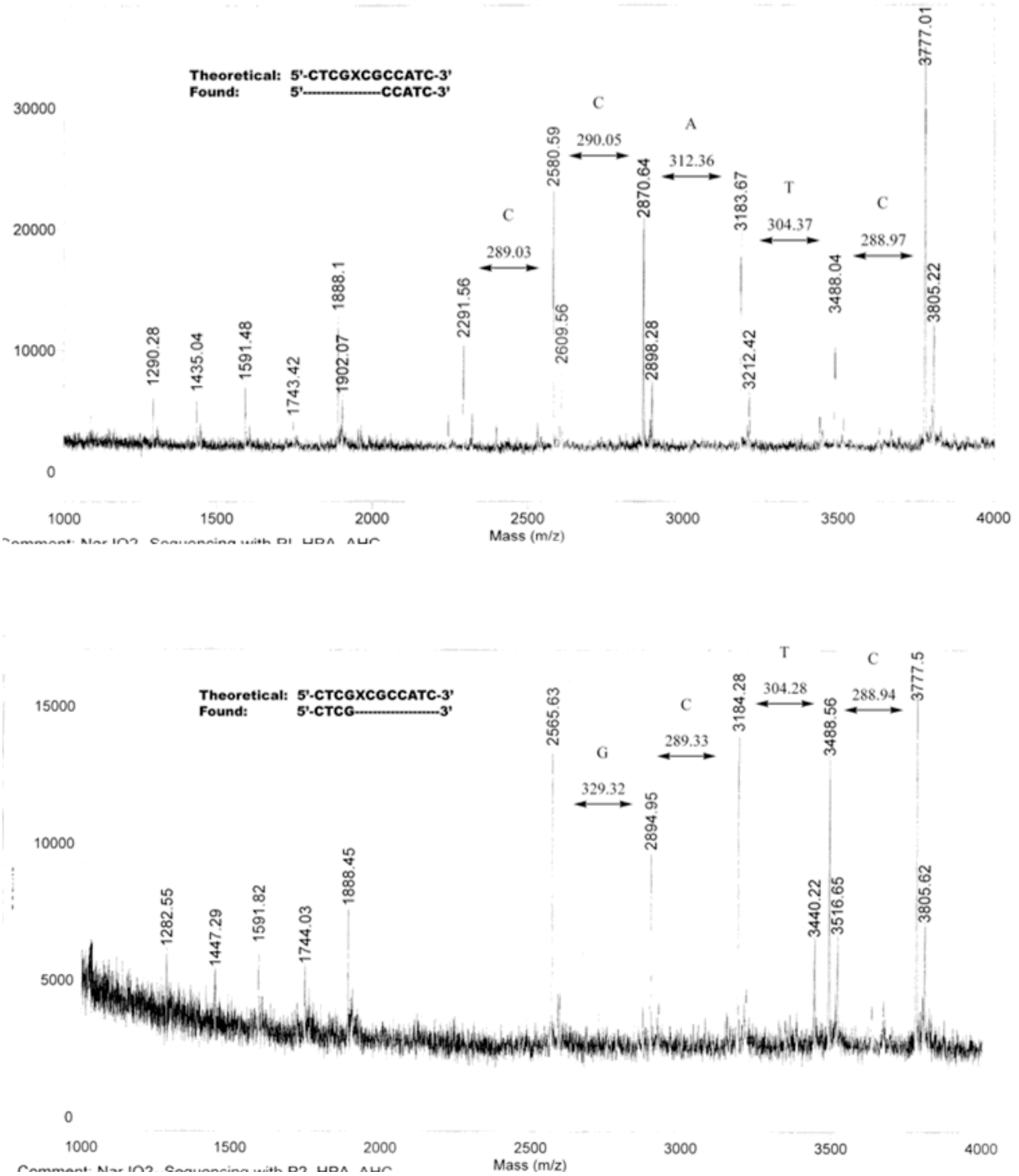

Figure S16. Sequencing of 5'-d(CTCG-G^{IQ}-CGCCATC)-3' (**3a**) by controlled digestion with phosphodiesterase I (top) or phosphodiesterase II (bottom) and MALDI-TOF analysis

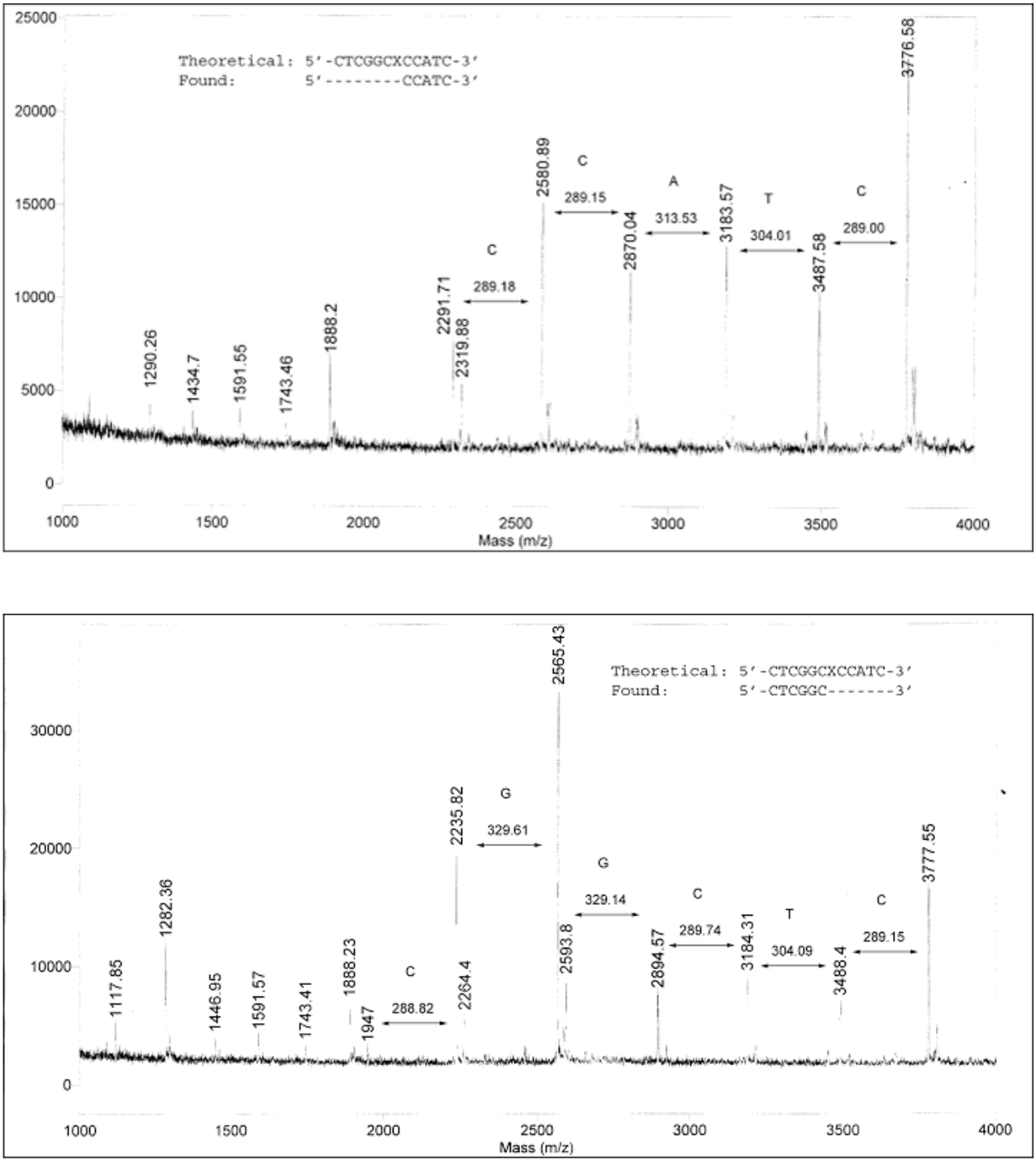

Figure S17. Sequencing of 5'-d(CTCGGC-G^{IQ}-CCATC)-3' (**4a**) by controlled digestion with phosphodiesterase I (top) or phosphodiesterase II (bottom) and MALDI-TOF analysis

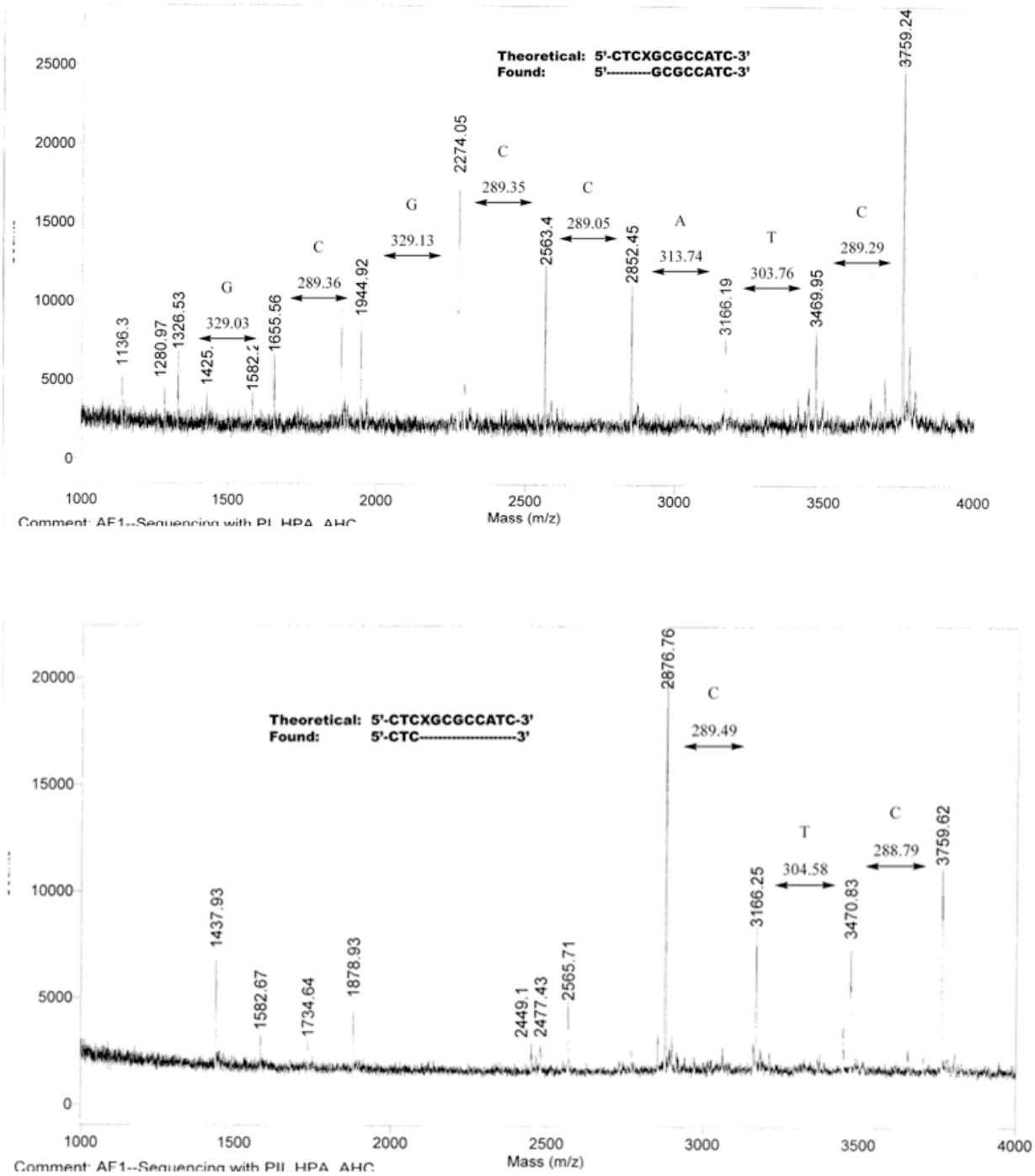

Figure S18. Sequencing of 5'-d(CTC-G^{AF}-GCGCCATC)-3' (**2b**) by controlled digestion with phosphodiesterase I (top) or phosphodiesterase II (bottom) and MALDI-TOF analysis

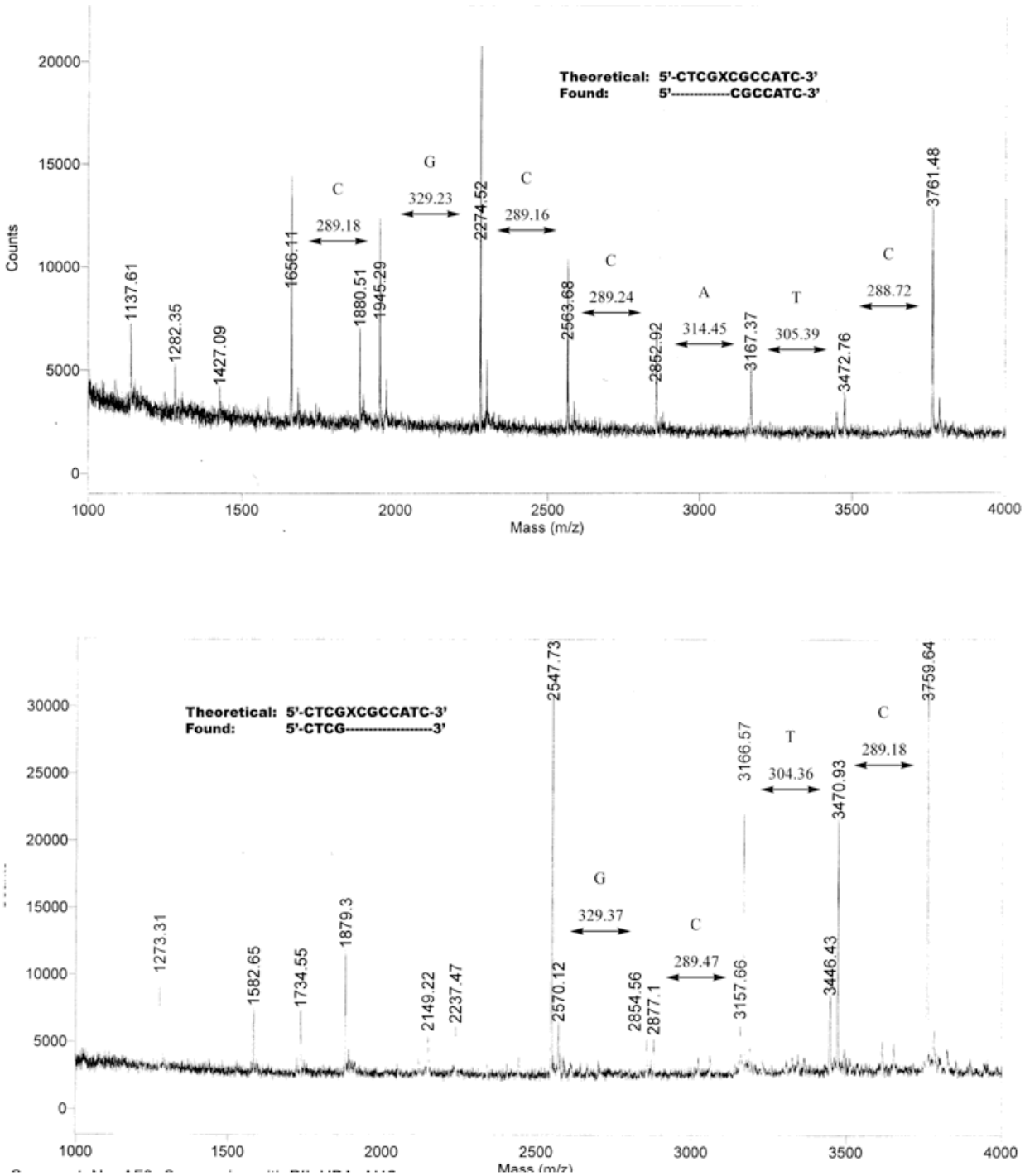

Figure S19. Sequencing of 5'-d(CTCG-G^{AF}-CGCCATC)-3' (**3b**) by controlled digestion with phosphodiesterase I (top) or phosphodiesterase II (bottom) and MALDI-TOF analysis

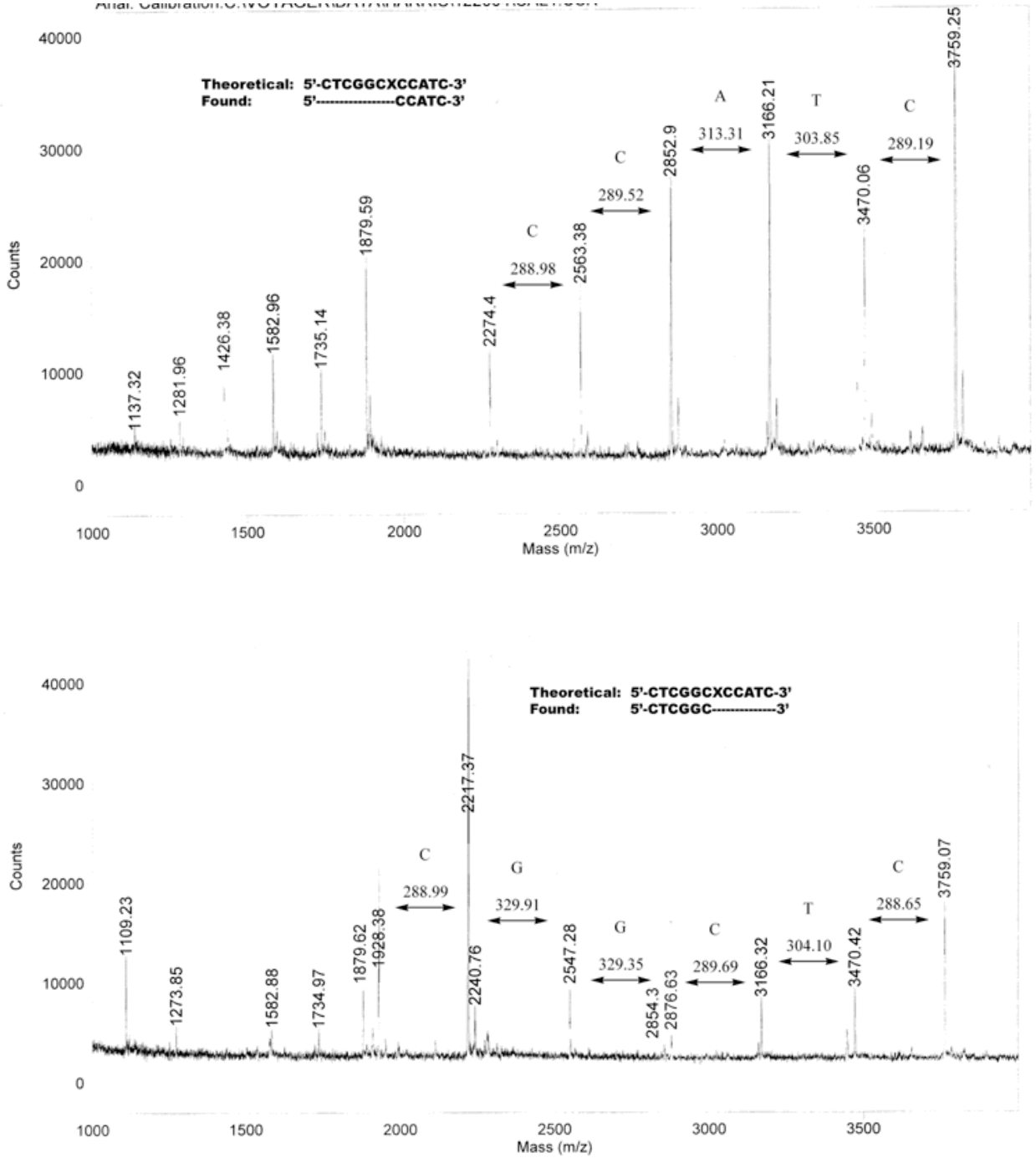

Figure S20. Sequencing of 5'-d(CTCGGC-G^{AF}-CCATC)-3 (**4b**) by controlled digestion with phosphodiesterase I (top) or phosphodiesterase II (bottom) II and MALDI-TOF analysis

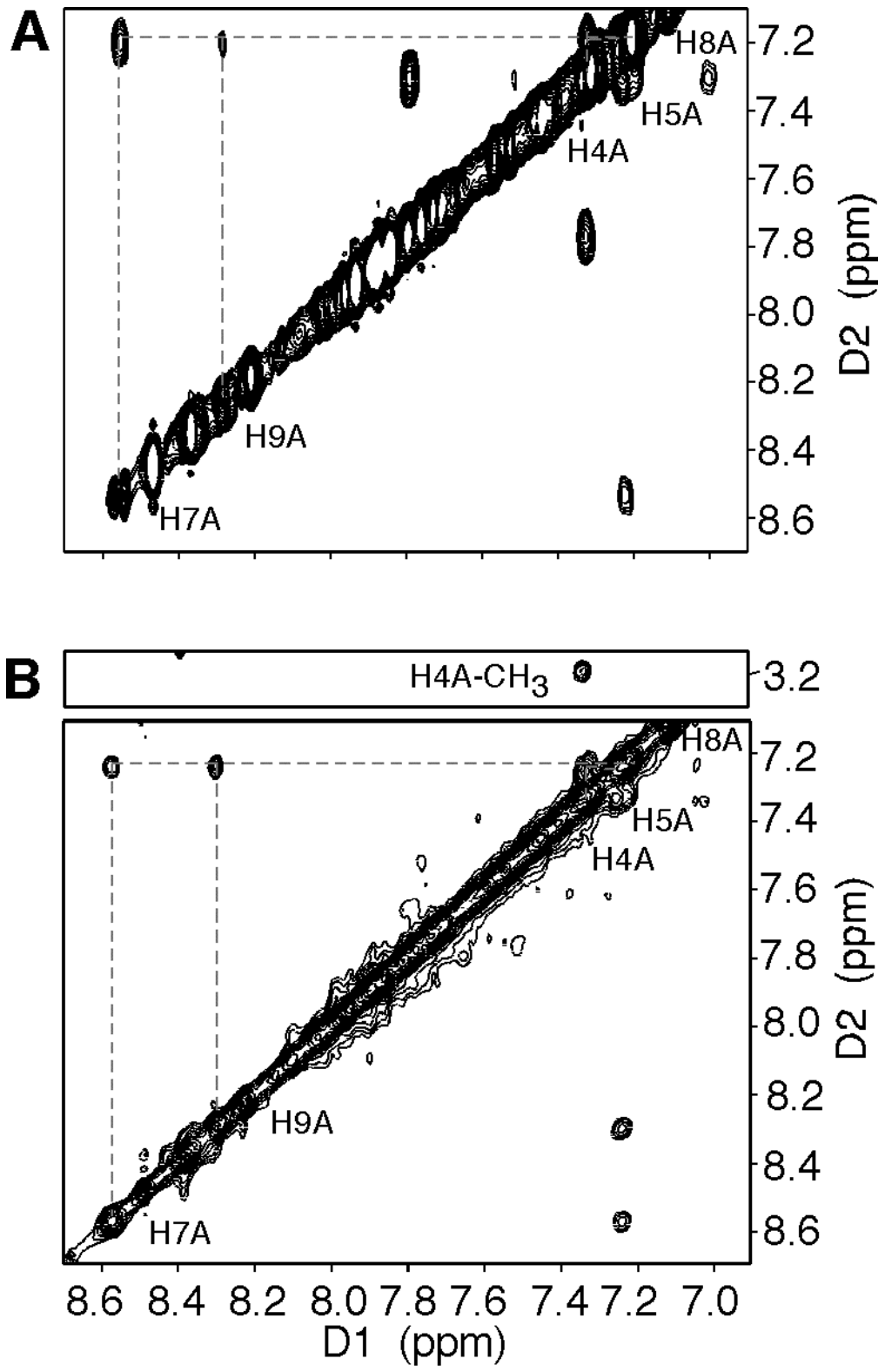

Figure S21. Expanded COSY (**A**) and NOESY (**B**) spectra of the IQ aromatic region of duplex **1a**

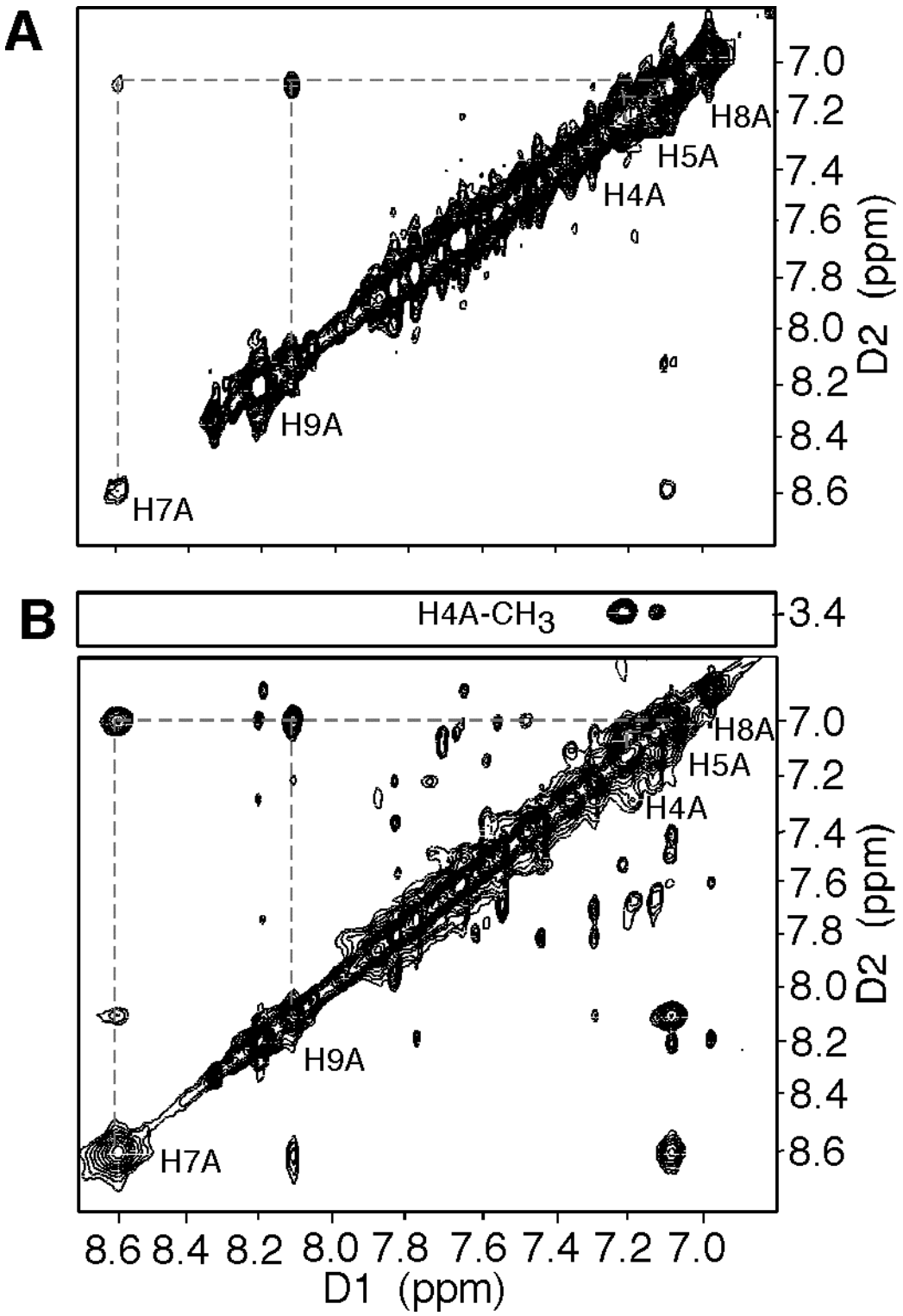

Figure S22. Expanded COSY (**A**) and NOESY (**B**) spectra of the IQ aromatic region of duplex **2a**

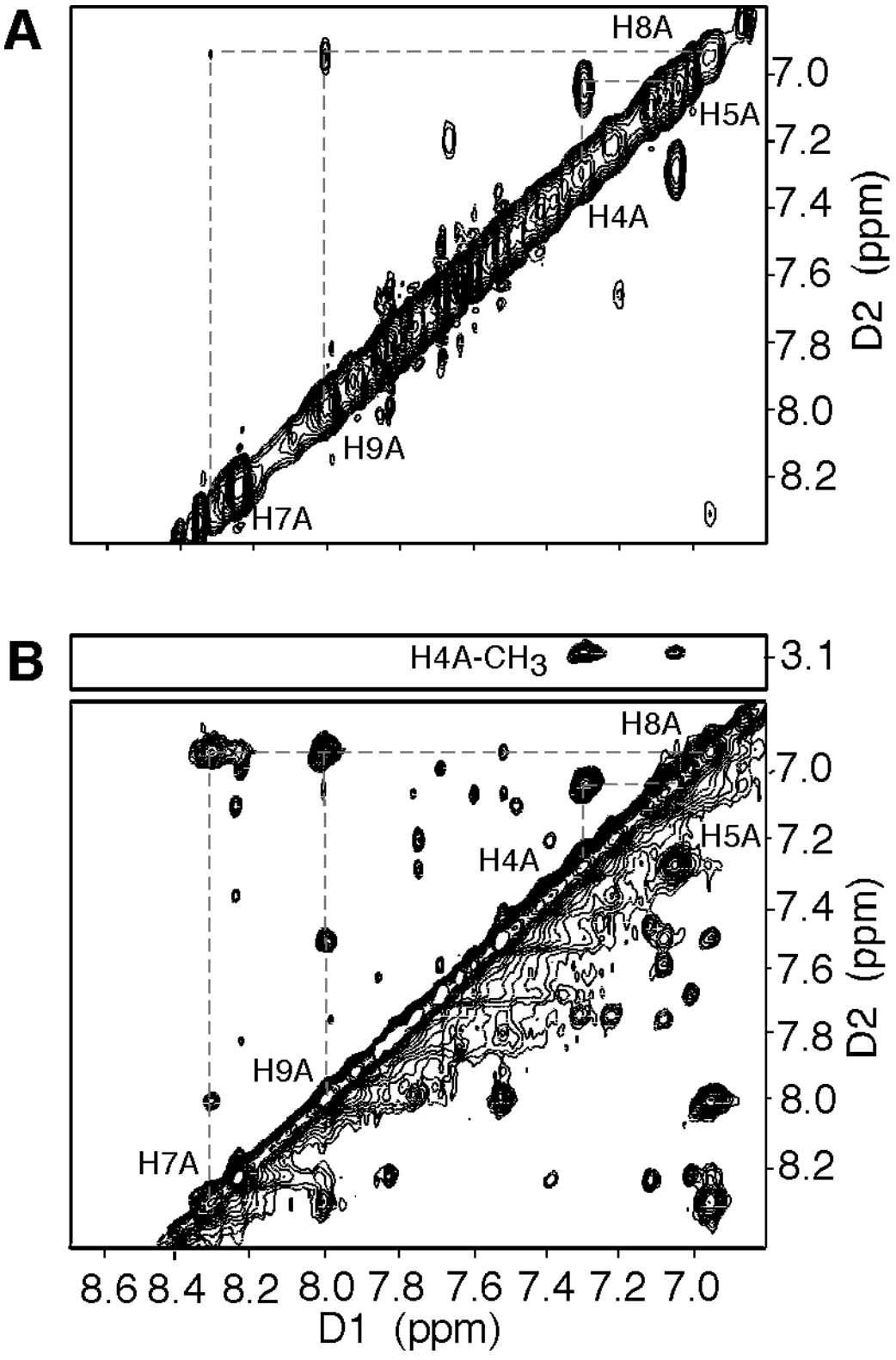

Figure S23. Expanded COSY (**A**) and NOESY (**B**) spectra of the IQ aromatic region of duplex **3a**.

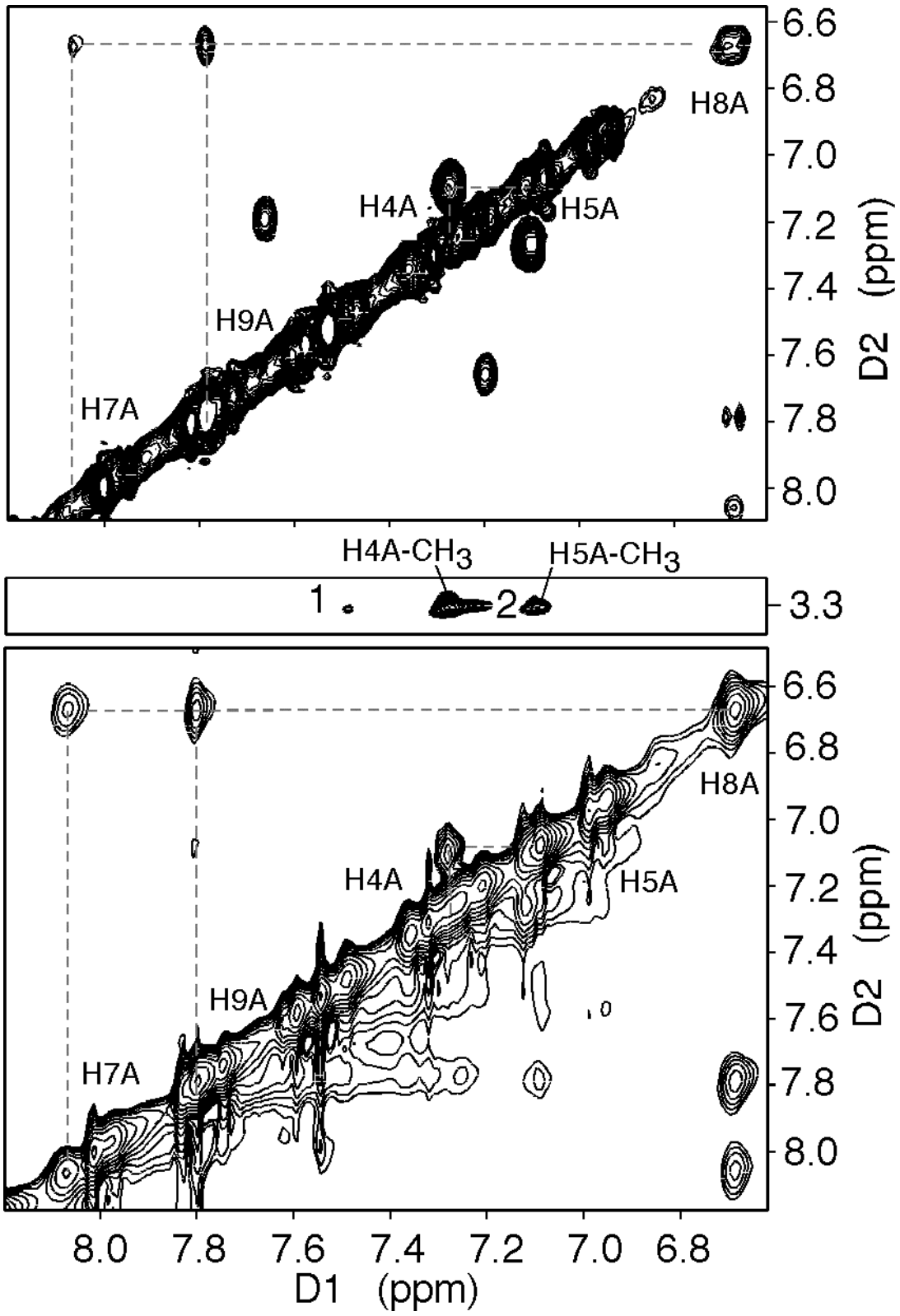

Figure S24. Expanded COSY (**A**) and NOESY (**B**) spectra of the IQ aromatic region of duplex **4a**, acquired at 25 °C with a mixing time of 200 ms.